Role of Caveolin-1 and Cholesterol in Transmembrane Fatty Acid Movement†

Tova Meshulam,‡,§ Jeffrey R. Simard,§,||,⊥ Jonathan Wharton,‡ James A. Hamilton,*,|| and Paul F. Pilch*,‡

Departments of Biochemistry, Biophysics, and Pharmacology and Experimental Therapeutics, Boston University School of Medicine, 715 Albany Street, Boston, Massachusetts 02118

Received October 3, 2005; Revised Manuscript Received December 8, 2005

ABSTRACT: We have created by transfection a series of HEK 293 cell lines that express varying amounts of caveolin-1 to test the possible effect of this protein on the transport and metabolism of long chain fatty acids (FA) in cells with this gain of function. We used an extracellular fluorescent probe (ADIFAB) to monitor binding of exogenous FA to the plasma membrane and an intracellular pH probe to monitor FA equilibration across the plasma membrane. Real-time fluorescence measurements showed rapid binding of oleic acid to the extracellular side of the plasma membrane and a rapid translocation across the lipid bilayer by the flip-flop mechanism (<5 s). Two cell lines expressing levels of caveolin-1 roughly comparable to that of adipocytes, which have a very high level of endogenous expression of caveolin-1, showed a relatively slow change in intracellular pH ($t_{1/2}$ < 100 s) in addition to the fast changes in fluorescence. We interpret this additional second phase to represent translocation of additional FA from the outer to inner leaflet of the plasma membrane. The slower kinetics could represent either slower flip-flop of FA across highly organized, rigid regions of the plasma membrane or binding of FA to caveolin-1 in the intracellular leaflet of the plasma membrane. The kinetics of palmitate and elaidate (a trans FA) transmembrane movement were identical to that for oleate. These results were observed in the absence of the putative FA transport protein, CD36, and in the absence of any changes in expression of fatty acid transport proteins (FATP) 2 and 4, and are in direct correlation with increased cellular free cholesterol content. FA metabolism was slow in all cell lines and was not enhanced by caveolin-1 expression. We conclude that transport of FA across the plasma membrane is modulated by caveolin-1 and cholesterol and is not dependent on the putative FA transport proteins CD36 and FATP.

Long chain fatty acids (FA)[1] serve a variety of needs in complex organisms, the vast majority of which involve energy storage and production. However, more recently appreciated roles for FA are as ligands for cell surface receptors (*1*) and as regulators of gene expression via their interaction with nuclear receptors (*2*). The fast rates of FA metabolism in many cells such as adipocytes require that they cross the plasma membrane quickly, entering or leaving the cell depending on the metabolic status of the organism. The mechanism(s) by which FA move through cell surface membranes remains unresolved. New biophysical approaches have on one hand provided evidence that passive diffusion (flip-flop) across the plasma membrane is very rapid and can account for cellular FA flux in the adipocyte (*3*) and on the other hand suggested that diffusion is not an adequate mechanism (*4*). However, all new biophysical approaches have shown that FA can enter adipocytes within seconds and can also leave rapidly.

Specific membrane proteins and/or transporters have also been implicated in the transport of FA through membranes, based in part on their ability to augment cellular FA uptake (including metabolism) when overexpressed. Such proteins include caveolin-1 (*5*), adipocyte cytosolic fatty acid-binding protein (aP2) (*6*), fatty acid translocase FAT/CD36 (*7*), plasma membrane-bound fatty acid binding protein ($FABP_{pm}$) (*8*), and members of the fatty acid transport protein (FATP) family (*9*, *10*). The FATP family members are acylCoA ligases (*11*) that may augment cellular FA uptake by virtue of their ability to convert FA to fatty acyl CoA derivatives and thus drive their transmembrane movement by creating an inward-directed gradient for FA diffusion (*12*, *13*). All of these proteins are expressed at significant levels in adipocytes, the major site where FA is stored in the fed state and mobilized for use in other tissues in the fasted state.

We previously employed adipocytes and plasma membrane vesicles derived from the adipocyte to study transmembrane FA movement. Oleic acid binds rapidly to the plasma membrane of adipocytes (*14*) with a partition coefficient similar to that of protein-free phospholipid vesicles (*15*). Using a dual-fluorescence technique, we showed that both binding and transmembrane movement of fatty acids occurred rapidly (<5 s) by a postulated diffusion mechanism (flip-flop) that was sufficiently rapid to support intracellular metabolism (*14*, *16*, *17*). The kinetics and the

† This work was supported by grants from the NIH to P.F.P. (DK-56935) and the American Diabetes Association and to J.A.H. from the NIH (HL-263435 and HL-67188).

* To whom correspondence should be addressed. P.F.P.: e-mail, ppilch@bu.edu; telephone, (617) 638-4044. J.A.H.: e-mail, jhamilt@bu.edu; telephone, (617) 638-5048.

‡ Department of Biochemistry.

§ These authors made equal contributions to the manuscript.

|| Department of Biophysics.

⊥ Department of Pharmacology and Experimental Therapeutics.

[1] Abbreviations: HEK, human embryonic kidney; FA, long chain fatty acid(s); SM, sphingomyelin; FATP, fatty acid transport protein; FABP, fatty acid binding protein.

10.1021/bi051999b CCC: $33.50
Published on Web 02/07/2006

partitioning suggested a high avidity of FA for the lipid bilayer such that competition by protein-mediated transport processes would be minimal. While this study and other studies (*18*−*20*) clarified that proteins are not required for FA transport, they do not exclude a role of the putative transport proteins in trafficking of FA in membranes or the direct or indirect participation in FA metabolism. However, studies to date have not revealed any mechanisms by which proteins influence transport of FA in the plasma membrane, other than by converting the FA to acyl-CoA, which cannot escape the cell (*12*, *13*, *21*, *22*).

Caveolin-1 is the most abundant of the putative FA binding proteins in adipocytes. It serves as a structural constituent of the caveolae that cover up to 20% of the adipocyte cell surface (*23*−*25*). Indeed, caveolin/caveolae expression is markedly induced during adipocyte differentiation from fibroblasts to mature fat cells (*26*, *27*). Caveolae are non-clathrin-coated plasmalemmal invaginations, which are also abundantly located on the surface of endothelial cells and smooth and striated myocytes (*28*). Caveolae make up a subclass of lipid rafts, characterized by their resistance to solubilization by Triton X-100 at 4 °C, their light buoyant density, and their enrichment in cholesterol and sphingolipids (reviewed in ref *28*). Postulated caveolae-mediated functions include a role in vesicular transport via endocytosis/transcytosis in endothelium and other tissues (*29*−*33*) and cellular cholesterol flux/homeostasis (*34*). Caveolae have also been suggested to play a role in signal transduction by serving as organizing centers for a variety of receptors and signal-transducing molecules (*35*). Importantly, caveolin-1, one of four proteins produced from three caveolin genes, has been implicated in the binding and/or transport of FA (*5*).

Thus, we sought to develop an experimental cell system to study the involvement of caveolin/caveolae in the transport of FA in the plasma membrane of cells that lack some of the putative FA transporters and have relatively limited FA metabolism on the time scale of FA transport from the extracellular medium to the cytosol. HEK 293 cell lines have virtually no endogenous caveolin-1 and lack the most common putative FA transport protein, FAT/CD36 (*7*), which is concentrated in caveolae in adipocytes and other cells (*36*−*38*). We created several cell lines expressing different levels of caveolin-1, the highest level approaching that observed in adipocytes. We found a threshold effect of caveolin-1 expression on plasma membrane cholesterol content: a moderate increase in the level of caveolin-1 expression resulted in no significant increase in the level of plasma membrane cholesterol, but higher levels of caveolin-1 expression increased the level of surface cholesterol by ~70% (ref *39* and Figure 3). This increase in the level of PM cholesterol was mirrored by alterations in the membrane transport of FA independent of any significant changes in FA metabolism or changes in the expression of putative FA transport proteins other than caveolin-1. Our data support a role for plasma membrane cholesterol and caveolin-1 in modulating the dynamics of FA in membranes in the absence of other protein facilitators.

MATERIALS AND METHODS

Materials. Oleic acid (99% pure) and all buffer materials were purchased from Sigma (St. Louis, MO). ADIFAB, BCECF-AM, and *cis*-parinaric acid were purchased from Molecular Probes (Eugene, OR). [^{14}C]Oleic acid and TLC lipid standard were purchased from NuChek Prep (Elysian, MN). Uniplate Silica Gel G TLC plates (scored 20 lanes × 20 cm) were obtained from Analtech Inc. (Newark, DE).

Buffers. MOPS-KRB buffer [20 mM MOPS, 118 mM NaCl, 5 mM KCl, 1.1 mM $MgSO_4$, 1.1 mM KH_2PO_4, 2.5 mM $CaCl_2$, and 5.1 mM glucose (pH 7.4)] was used in the preparation of cultured HEK cells and all fluorescence measurements.

Fatty Acid Stock Solutions. Oleate was dissolved in chloroform, which was evaporated under N_2 gas for an accurate determination of its dry weight. After evaporation of the solvent, the dried oleate was dissolved in enough 1 mM KOH to produce a 10 mM stock of fatty acid. If needed, 0.1 mM KOH was added dropwise to increase the pH to >10 to ensure complete dissolution of the FA as micelles. FA stock solutions were also made by dissolving oleate in DMSO and ethanol. *cis*-Parinaric acid was dissolved in DMSO to produce a 40 mM stock.

HEK 293 Cell Lines and Transfection (39). cDNA for mouse caveolin-1α was produced by RT-PCR from 3T3-L1 adipocytes. The cDNA was then inserted into the pcDNA3.1 hygro vector and transfected into HEK 293 cells using Lipofectamine 2000 from Invitrogen (Carlsbad, CA) according to the manufacturer's instructions. Single colonies were selected using cloning rings (Falcon), and each produced line of HEK 293 cells was tested for levels of caveolin-1 expression. Four cell lines with different levels of expression of caveolin-1 were developed from this procedure. The five cell lines that were studied, starting from little to no expression of caveolin-1 ranging to a high level of expression of caveolin-1, are Parent, D20, D7, A4, and B8. All cell lines were grown in Dulbecco's modified Eagle's medium (DMEM) from Mediatech Inc., (Herndon, VA), containing a mixture of penicillin (5000 units/mL) and streptomycin (5000 μg/mL) from Invitrogen. The medium was supplemented with 5% fetal bovine serum (FBS) (Hyclone) and 5% calf serum (CS) (Invitrogen).

Caveolin Biotinylation in HEK 293 Cells. The B8 cell line was exposed to 1 mM EZ-Link-sulfo-NHS-SS-biotin (Pierce) for 5 min as we have previously described (*40*). Alternatively, enriched plasma membranes, obtained from B8 cells and prepared as we described previously (*39*), were incubated with 0.1% Triton X-100 for 15 min at 4 °C and then biotinylated as described above. The cross-linking reaction was quenched by the addition of an ice-cold buffer consisting of 20 mM Tris and 25 mM ethanolamine (pH 7.4). Biotinylated proteins were adsorbed onto immobilized avidin, eluted with dithiothreitol, and subjected to SDS−PAGE and Western blotting with anti-caveolin-1 antibody (*37*) as we described in ref *40*. Protein amounts were determined using a BCA kit from Pierce (Rockford, IL), and equal amounts were analyzed (Figure 2B).

Antibodies and Western Blotting. Antibodies for caveolin-1, flotillin-1, and SSAO were obtained from BD Transduction Laboratories (Lexington, KY). Antibodies to the FATPs were a kind gift of A. Stahl (Stanford University, Palo Alto, CA). Primary antibodies were detected using secondary antibodies conjugated to horseradish peroxidase from Sigma and chemiluminescence substrate from PerkinElmer Life Sciences (Boston, MA).

Immunofluorescence. HEK cells were grown in six-well tissue culture plates containing poly-L-lysine-coated cover slips (Becton Dickinson, Franklin Lakes, NJ) for 48 h. Cells were then washed one time with PBS and fixed with 3.7% formaldehyde in PBS for 15 min at room temperature and then washed two more times with PBS. Cells were blocked and permeabilized by incubation with buffer P [5% donkey serum (Sigma), 5% bovine serum albumin, and 0.5% Triton X-100 in PBS] for 20 min at room temperature. The fixed cells were incubated for 2 h with rabbit anti-caveolin-1 antibody at a dilution of 1/250 in buffer P at room temperature. Four more washes with buffer P were then performed, and the cells were covered in aluminum foil and incubated for 30 min at room temperature with an anti-rabbit Cy3 secondary antibody (Jackson ImmunoResearch Laboratories, Inc., West Grove, PA) at a dilution of 1/250. Again, the cells were washed four times with PBS, and they were then mounted with a glycerol/PBS solution (component A of the SlowFade Antifade Kit from Molecular Probes). The stained cells were observed with a Zeiss Axiovert 200M microscope equipped with a Hamamatsu Photonics K.K. camera for standard immunofluorescence.

Determination of the Total and Unesterified Cholesterol Content. The assays were performed as outlined previously (*41*). Briefly, the total amount of cellular cholesterol was estimated by extracting lipids from HEK cells by the Folch method (*42*), and the lipid phase was hydrolyzed with KOH and ethanol. A colorimetric assay (horseradish peroxidase) was used for detection. For estimation of the amount of unesterified cholesterol, the same assay was used but without the hydrolysis step.

Preparation of Cultured HEK Cells for Fluorescence Measurements. HEK cells were incubated with 0.125 μg/mL (200 nM) BCECF-AM for 30 min at 37 °C and washed twice in 20 mM MOPS KRB buffer (pH 7.4). Cells were resuspended in buffer following a 10 s treatment with 0.1% trypsin-EDTA (Invitrogen).

Fluorescence Measurements. Fluorescence measurements were taken using a Spex Fluoromax-2 instrument from Jobin Yvon (Edison, NJ). The ratiometric fluorescence of BCECF was measured using excitation at 439 and 505 nm ($R = ex_{505}/ex_{439}$) with an emission of 535 nm. The ratiometric fluorescence of ADIFAB was measured using excitation at 386 nm and emission of 432 and 505 nm ($R = em_{505}/em_{432}$). The emission of *cis*-parinaric acid was measured at 416 nm after exciting the probe at 320 nm. In experiments in which the binding and flip-flop of fatty acids into cultured HEK cells were monitored, the fluorescence signals of each probe (ratiometric or single λ emission) were measured alone or simultaneously as oleate was added through the injection port above the cuvette in the absence of BSA (60 nmol of FA/cuvette = 20 μM final concentration). All samples were rapidly stirred throughout each experiment to ensure rapid mixing of the fatty acids with cells. The surface of the sample changer was also warmed to 37 °C by a flow of water pumped into the sample compartment from a temperature-controlled external water bath. The effect of caveolin expression on FA-induced pH changes was assessed by measuring the level of binding to the plasma membrane, the magnitude of the pH drop, and the length of time over which that drop occurred. Vehicle alone, DMSO or KOH, added at a >1/500 dilution to the external buffer did not affect the intracellular pH.

HEK 293 cells (Parent and B8 cell lines) containing 2 μM BCECF were permeabilized to H^+ with nigericin (1 μg of nigericin/1 mg of PC) such that $pH_{in} = pH_{out}$ at all times. The pH_{out} was measured with a pH mini-electrode (Microelectrodes, Bedford, NH) and was titrated with small volumes of 8 M KOH and H_2SO_4. The ratiometric excitation of BCECF was recorded at each pH value to generate a calibration curve. The fluorescence of BCECF was linear between pH 6 and 8 and indistinguishable for the cell lines expressing a negligible (Parent) or high level of caveolin-1 (B8).

Measurement of the Intracellular Fatty Acid Metabolism. Cells were prepared and isolated as previously described for fluorescence measurements. [^{14}C]Oleate (20 μM) was added to 3 mL of a cell suspension in a test tube, rapidly mixed, and placed in a shaking 37 °C water bath for 0, 2, 5, 15, 30, or 45 min. After incubation, the suspension of cells was poured into 1 mL of "stop solution" (40/10/1 hexane/2-propanol/sulfuric acid mixture) to lyse the cells and extract the lipid products. Samples were then centrifuged (20 min at 1000 rpm) after being washed with 3 mL of deionized water followed by 2 mL of hexane to extract all lipids into the organic layer. The hexane layer was then removed, air-dried, and resuspended into 100 μL of a chloroform/methanol mixture (1/1). Approximately 50 μL of lipid mixture was then placed on silica TLC plates along with 20 μL of lipid standard (monoglyceride, diglyceride, triglyceride, free fatty acid, and cholesterol ester), dried under N_2 gas, and placed in a solvent tank containing 1 L of "running buffer" (80/20/1 hexane/ethyl ether/acetic acid mixture). The solvent was allowed to move up the plate to within 1 cm of the top. The plate was removed from the tank, air-dried in the hood, and placed in a second sealed tank to develop in the presence of iodine flakes. Different lipid bands were marked and then scraped into individual scintillation vials along with 4 mL of Ecoscint solution to measure the radioactivity. The amount of each lipid species extracted was calculated at each time point as a percentage of the total lipids extracted.

RESULTS

Characterization of HEK Cells Expressing Caveolin-1. We confirmed by indirect immunofluorescence that expressed caveolin-1 was directed to the cell surface (Figure 1). Representative fields from the two cell lines expressing the highest levels of caveolin (B8 and A4) as well as those expressing intermediate levels (D7 and D20) and the lowest levels of caveolin-1 (Parent) are shown. There was little or no detectable cell surface fluorescence in the latter cell line, as was previously shown for the case of the parental HEK 293 cells (*39*), whereas the other cell lines showed a distinct pattern of fluorescence around the rim (surface) of the cells. Thus, as expected and as shown by others for caveolin-1 transiently transfected into HEK cells (*25*), this protein was largely expressed at the cell surface. To confirm that caveolin-1 was inserted into the inner leaflet of the plasma membrane bilayer (*43*), the B8 cell line cell surface was biotinylated with a membrane impermeable reagent (*40*), and alternatively, the isolated plasma membrane was reacted with the same reagent after its solubilization (Figure 1B). Bioti-

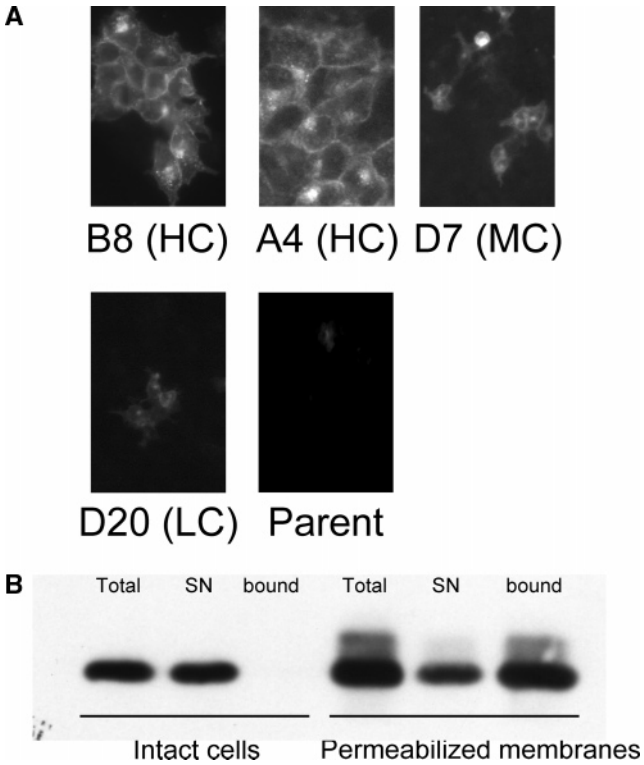

FIGURE 1: Caveolin-1 is directed to the inner surface of transfected HEK cells as determined by indirect immunofluorescence and vectorial biotinylation. (A) Representative fields from the two cell lines expressing the highest levels of caveolin-1 (HC) (B8 and A4) as well as the medium level of caveolin-1 (MC) (D7) and the lowest level of transfected caveolin-1 (D20) are shown. HEK cells were fixed and probed with polyclonal anti-caveolin-1 antibody followed by Cy-3 conjugated to donkey anti-rabbit antibody as described in Materials and Methods. The stained cells were viewed in a Zeiss Axiovert 200M microscope equipped with a Hamamatsu Photonics KK camera for immunofluorescence. (B) Intact cells (B8) (left three lanes) or permeabilized membranes from these cells (right three lanes) were biotinylated, and labeled proteins were isolated and subjected to SDS−PAGE and Western blotting as described in Materials and Methods. Depicted is a representative blot, one of three independent experiments.

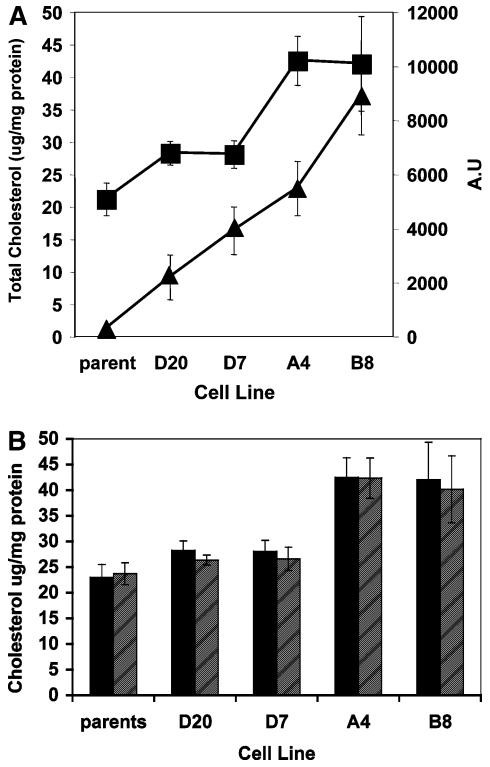

FIGURE 2: Cells expressing higher levels of caveolin-1 have higher levels of free cholesterol. (A) Membranes from transfected HEK293 cells were subjected to SDS−PAGE and immunoblotted using anti caveolin-1 antibody as described in the legend of Figure 1. Images were scanned, and quantitative analysis was performed using National Institutes of Health (NIH) image 1.63 software; the values that were obtained (▲) were expressed in arbitrary units (AU). Cells were Folch extracted, and total cholesterol was quantified (■) as outlined in Materials and Methods. (B) HEK 293 cells lines expressing different levels of caveolin-1 were Folch extracted, and total and unesterified cholesterol was quantified as outlined in Materials and Methods. Filled bars depict data for total cholesterol, and hatched bars depict data for unesterified cholesterol. Data in panels A and B are means ± the standard deviation of three independent experiments.

nylated proteins from membranes for each condition were isolated on an avidin column and, following elution and SDS−PAGE, were blotted for caveolin-1. As shown in Figure 1B, >80% of this protein is biotinylated when the inner leaflet is accessible to reagent and none when intact cells were employed. The small degree of smearing (right panel) likely represents biotinylation of multiple amino groups on a given caveolin-1 molecule.

Transfection of caveolin-1 in other cell types has been shown to lead to an increase in the level of free cholesterol (*44*). Thus, we investigated whether HEK cells expressing different levels of caveolin have different levels of cholesterol. Cells expressing low (parental) or intermediate levels (D20 and D7) of caveolin-1 had statistically indistinguishable levels of total cholesterol (Figure 2). In contrast, cells expressing high levels of caveolin (A4 and B8) had 60−70% higher levels of cholesterol than the parental and other cell lines ($p < 0.005$) (see also ref *39*). These data suggested that there is a threshold level of caveolin-1 required for an increase in the level of cellular cholesterol. The levels of total and unesterified cholesterol were the same in these cells (Figure 2B), so the increased level of cholesterol that was correlated with caveolin expression levels represents free cholesterol, 80−90% of which is known to be at the plasma membrane depending on the cell type (*45*).

Effect of Caveolin-1 and Cholesterol on the Transport of FA in the Plasma Membrane. We used two fluorescence approaches to monitor FA transport in the plasma membrane. Both measurements are made in real time without separation procedures. FA is added in the absence of albumin to prevent the confounding factors of desorption of the FA from albumin and the partition of FA to the membrane (i.e., how fast can albumin release FA and how much is delivered to the cell at any given time point).

The first measurement used a pH dye (BCECF) trapped in the cytosol to detect protons released by FA that cross the membrane by diffusion (flip-flop). We established that the response of the dye within the cell was linear with pH in the pH range of our studies (Materials and Methods) so that the changes in fluorescence can be attributed to changes in intracellular pH. Addition of oleic acid to the external medium of a suspension of cells resulted in an immediate and rapid (<2 s) decrease in fluorescence. All cell lines exhibited this initial rapid pH decrease, which is similar to that reported with the same protocols for adipocytes in suspension (*14*). The magnitude of this fast component was

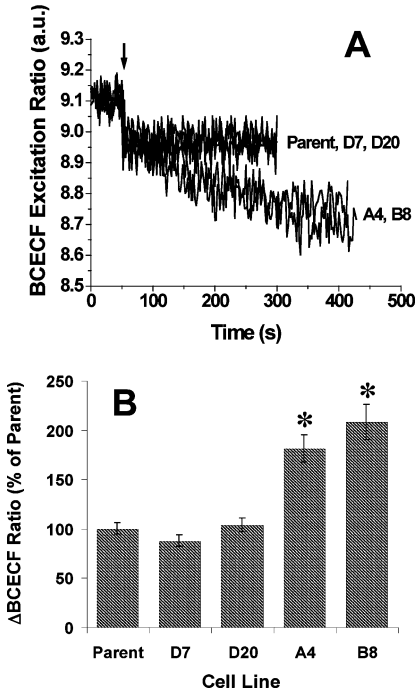

FIGURE 3: Elevated levels of caveolin-1 increase the extent of fatty acid uptake into HEK 293 cells. The change in BCECF fluorescence was measured in response to a single dose of oleate (20 μM, arrow) as described in Materials and Methods. An initial rapid pH drop (<2 s) was observed for all cell lines. Cells expressing high levels of caveolin-1 also produced an additional slow component of fluorescence change. (A) The data are representative fluorescence traces from different cell lines. The total change in BCECF fluorescence observed in A4 and B8 cell lines was significantly greater than that observed in Parent, D7, or D20 cell lines ($p < 0.0001$). (B) The percent fluorescence change is shown for each cell line compared to that of the Parent cells on the same day at 400 s. The means ± standard errors of 13 independent experiments are shown for all cell lines.

the same despite the varying amounts of caveolin-1 expression and membrane cholesterol content. None of the cell lines showed a rapid recovery of the intracellular pH, which is seen for adipocytes with similar additions of oleic acid (*14*). In fact, an additional relatively slow decrease in pH was seen in cells expressing high levels of caveolin-1 (Figure 3A). The total decrease in fluorescence following addition of a single dose of oleic acid (20 μM) significantly increased with the amount of caveolin-1 expressed in each cell type (Figure 3B). These data were analyzed with a one-way analysis of variance (ANOVA), the results of which revealed a significant main effect [$F(4,60) = 24.079$, $p < 0.0001$]. Subsequent post-hoc analyses (Tukey's HSD, $p < 0.05$) showed that the A4 and B8 groups were significantly different from the Parent group. Cells expressing intermediate levels of caveolin-1 (D7 and D20) gave results similar to those of Parent cells, while both groups of caveolin-1-rich cells (A4 and B8) produced decreases in fluorescence that were nearly doubled in magnitude.

Repeated sequential additions of FA produced pH changes that were dose-dependent up to the maximum added [60 μM oleate (20 μM/addition)] (Figure 4A). Additionally, the total pH drop resulting from three additions of FA was linear with FA concentration up to 60 μM in all cell lines (Figure 4B). The total pH drop at 60 μM FA was greater for caveolin-rich cells (B8), which produced larger reductions in cytosolic pH with each cumulative addition of FA. The total pH drops measured in Parent and intermediate-expressing caveolin-1 cells were not significantly different.

To determine whether the results of Figure 3 were specific to oleate, we performed uptake experiments by measuring changes in intracellular pH in response to saturated (palmitic) and mono-unsaturated trans FA (elaidic, C18:1). Palmitate was chosen over stearate because it is much more soluble than stearate. As shown in Figure 5, the fluorescence data for these two FA are qualitatively identical to those obtained for oleate. Both show a single, rapid phase of pH change in parental cells and a second slow phase in the B8 cell line (Figure 5). Although the time required for completion of the pH change observed in B8 cells was slightly different in each experimental trial, the magnitude and rate of the pH change were the same for oleate as they were for the two additional FA that were tested. Thus, three structurally distinct FA show essentially identical behavior with regard to transmembrane movement in our cell system.

Our second fluorescence approach used ADIFAB, a fluorescently labeled FA binding protein, to monitor binding of FA to the plasma membrane. It was important to measure this step exclusively because intracellular pH changes caused by FA influx across the plasma membrane are the result of binding of FA to the external leaflet and translocation of

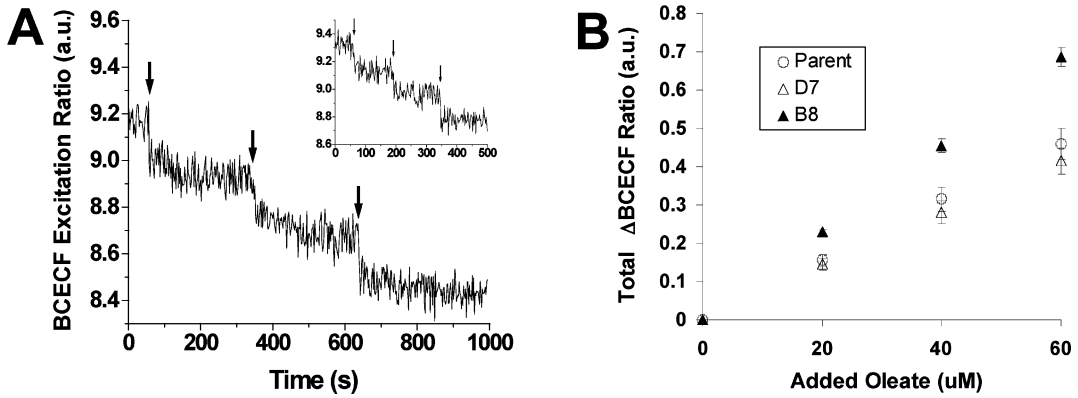

FIGURE 4: Fatty acid diffusion into HEK 293 cells is dose-dependent in cells expressing low and high levels of caveolin-1. The change in BCECF fluorescence was measured in response to three sequential doses of oleate (20 μM, arrows). Each dose produced pH drops of similar magnitude in B8 cells and Parent cells (inset). (A) The total pH drop resulting from each sequential dose of oleate was linear up to a total of 60 μM oleate. (B) The total change in BCECF fluorescence was greatest in cells expressing high levels (▲, B8) of caveolin-1. Cells expressing low (○, Parent) and intermediate (△, D7) levels of caveolin-1 showed similar changes in BCECF fluorescence. Data in Panel B are means ± standard deviations of three independent experiments.

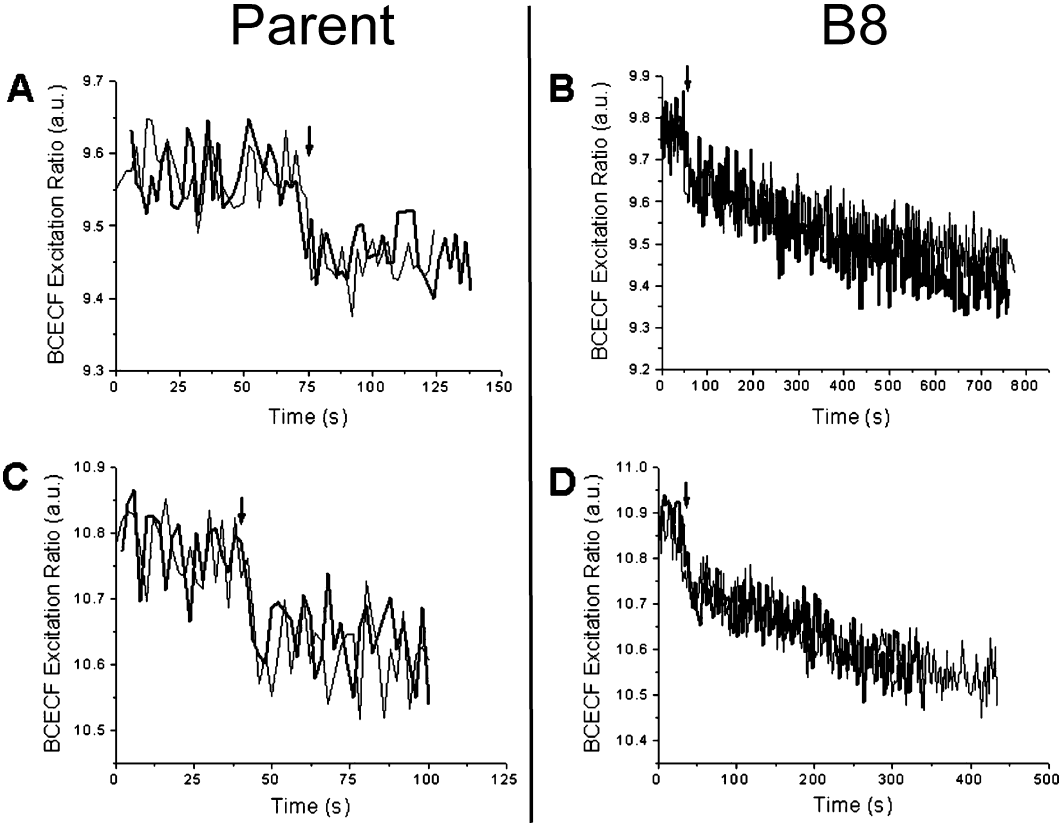

FIGURE 5: Movement of FA into HEK cells is independent of FA structure. The intracellular pH changes (thin line) generated by addition (arrow) of 20 μM palmitate (A and B) and 20 μM elaidate (C and D) to Parent (A and C) and B8 cells (B and D) were measured as in Figure 3 and compared to that for oleate (thick line) measured at the same time. The traces shown are representative of four such independent experiments. Note the different time scales for completion of the pH change in Parent and B8 cells.

some of the FA (in its un-ionized form) across the bilayer. The slow component of intracellular acidification monitored by the BCECF dye could be caused by either slow binding or slow translocation. When added to the external buffer, ADIFAB reports both the kinetic and thermodynamic components of adsorption of FA to the extracellular face of the plasma membrane (*46*). As shown in Figure 6, addition of a single dose of oleic acid (20 μM) to cells expressing low and high levels of caveolin was accompanied by a rapid increase in ADIFAB fluorescence to a maximal value (<2 s), indicating equally rapid binding of FA to the lipid bilayer in both cell lines (Figure 6A,B). The magnitude of this increase is directly proportional to the concentration of FA that binds to the plasma membrane (*14*).

A slow decrease in ADIFAB fluorescence was observed after the maximal increase. In cells with a low level of caveolin-1, this return of ADIFAB fluorescence was first-order (6B), but in cells with a high level of caveolin-1, we observed a slower second phase of decreased ADIFAB fluorescence (Figure 6A). The decrease in ADIFAB from its maximal value could represent several events (see Discussion and Figures 9 and 10), including intracellular metabolism of oleic acid (*14*). To investigate the potential contribution of metabolism of the added FA, we replaced oleate with *cis*-parinaric acid (PA), a natural FA that is not metabolized by cells. Addition of 80 μM *cis*-parinaric acid was accompanied by a very rapid increase in ADIFAB fluorescence (similar to that for oleic acid) but with a smaller decrease from its maximal value (Figure 6C).

This result with PA suggested that some, but not all, of the decrease in ADIFAB fluorescence after the addition of oleic acid could be attributed to FA metabolism. Accordingly, we performed metabolic tracer studies employing [^{14}C]oleate to quantify its incorporation into intracellular lipids by TLC analysis as a function of time. The disappearance of unesterified oleic acid and the appearance of esterification products were much slower than for adipocytes, which with a similar experimental protocol esterified most of the exogenously added oleic acid within 5 min (*14*). Parental HEK cells metabolized oleate somewhat faster than caveolin-1-rich cells at later time points, but there were no significant differences in oleate metabolism among the different cells at the 5 min time point (Figure 7) where cells show differences in intracellular pH changes (Figures 4−6). The slightly enhanced metabolism of oleic acid in Parent cells suggests that FA metabolism does not account for the greater pH decrease in high-caveolin/cholesterol level cell lines. However, it is possible that the ectopic expression of caveolin-1 leads to alterations in the level of putative fatty acid transporters, such as CD36 and members of the FATP family. As noted earlier, there is no CD36 expression in HEK 293 cells (ref *47* and RT-PCR data not shown). The FATP proteins that are known to be expressed in kidney (*10*), namely, FATP2 and FATP4, were expressed in HEK cells but at a level that was independent of caveolin-1 expression (Figure 8A,B).

DISCUSSION

Fatty acids are used as metabolic fuel by all tissues, especially heart and resting skeletal muscle. FA are stored primarily in adipocytes in the form of triglycerides, which can be rapidly hydrolyzed to release FA in response to the

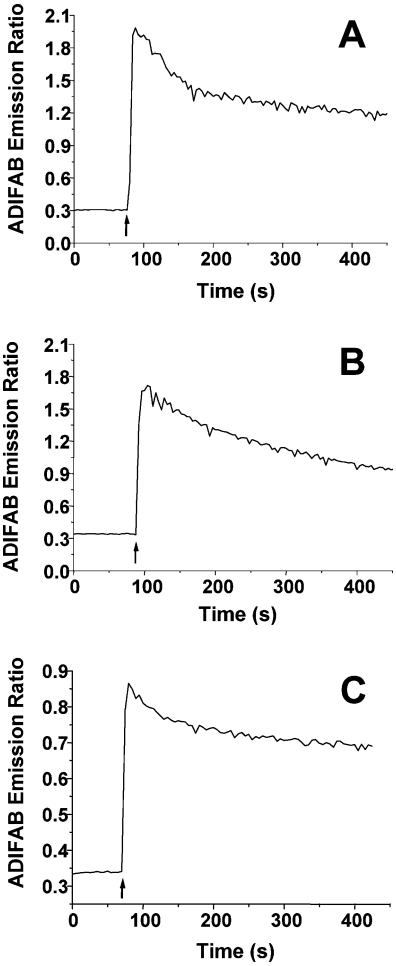

FIGURE 6: Fatty acids bind rapidly to HEK 293 cells expressing low and high levels of caveolin-1. The binding of fatty acids was assessed using the fluorescent probe ADIFAB, which was placed in the external buffer to monitor unbound concentrations of FA. The rapid increase in ADIFAB fluorescence indicates rapid binding of oleate (20 μM) to B8 (A) and Parent (B) cell lines (<2 s). The binding of *cis*-parinaric acid to B8 cells (80 μM) was also rapid (<2 s) as measured by ADIFAB fluorescence (C). A larger dose of *cis*-parinaric acid was required to achieve equivalent membrane partitioning because this fatty acid is more water soluble than oleate. The recovery of ADIFAB fluorescence measures the disappearance of FA from the external buffer that is in equilibrium with the plasma membrane as the FA is sequestered by the cell.

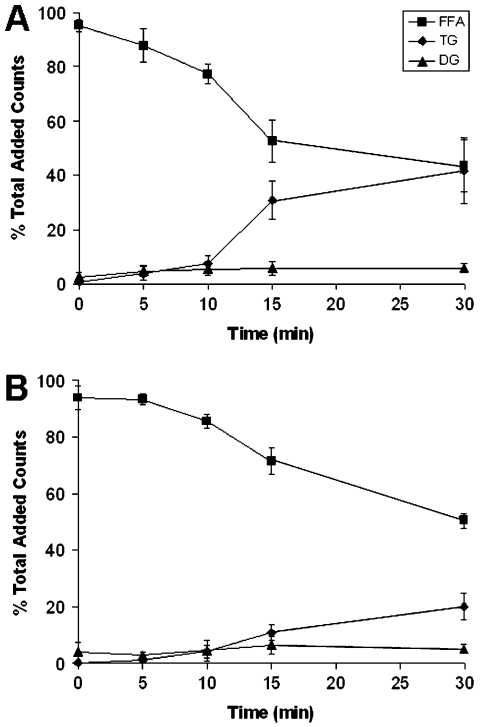

FIGURE 7: Metabolism of [^{14}C]oleate is slower in cells expressing high levels of caveolin-1. [^{14}C]Oleate was added to Parent and B8 cell lines, and lipids were Folch extracted after an incubation period of 0, 2, 5, 15, 30, or 45 min (data for 30−45 min not shown). Extracted lipids were purified by TLC to assess the incorporation of unesterified [^{14}C]oleate into MG, DG, TG, and CE. For the sake of simplicity, only free fatty acid (FFA) diglycerides (DG) and triglycerides (TG) are shown. Parent cells (A) metabolized FA significantly faster between 5 and 15 min than B8 cells (B). Metabolism was not significantly different between cell lines within the time scale of fluorescence measurements (0−5 min). The level of accumulation of MG and CE was not above background (data not shown). The data for FFA, DG, and TG are means ± standard deviations from four independent experiments.

metabolic demand of other tissues and organs. Thus, the bidirectional flux of FA across the plasma membrane occurs to a particularly large extent in adipocytes, and this begs the question of what mechanism(s) mediates this FA movement. The adipocyte plasma membrane has multiple proteins with postulated roles in modulating the transmembrane flux of FA. These include caveolin-1, FATP, FAT/CD36, and $FABP_{pm}$, as discussed in the introductory section. Moreover, entry of FA into fat cells and fat cell membrane vesicles is very rapid (*14*), on a time scale of seconds or less, the same as that for FA diffusion into and out of protein-free vesicles (*48*). Thus, we embarked on efforts to reconcile the roles of the above membrane proteins with the fast diffusion of FA across the plasma membrane of adipocytes (*14*), HepG2 cells (*49*), and HEK293 cells (this study). Interestingly, we report, for the first time, an additional slow phase of transmembrane FA movement that is caveolin- and cholesterol-dependent (Figure 3) and that we cannot ascribe to differences in cellular FA binding (Figures 6 and 9).

Thus, while adipocytes and hepatocytes are highly physiologically relevant for studying FA transport, they exhibit rapid FA metabolism (*14*, *49*). This, together with the presence in adipocytes of multiple membrane proteins capable of altering FA flux, makes the interpretation of FA uptake data difficult in these cell types. Therefore, we sought to create a simpler cellular system for studying FA transmembrane movement and chose HEK cells because they lack caveolin-1, CD36, and FATP1. In addition, HEK cells metabolize FA very slowly (Figure 7) compared to the time frame of transmembrane FA movement (Figures 3−5). Since caveolin-1 can bind FA directly (*5*) and is particularly abundant in adipocytes (*26*, *27*), we created a series of HEK cells that express caveolin-1 at various levels (Figures 1 and 2) and focused on the possible role of this protein in FA uptake. An additional rationale for this notion is that animals lacking caveolin have abnormally small adipocytes and aberrant FA metabolism (*50*). Finally, FA can reach potentially cytotoxic levels upon lipolysis in adipocytes, possibly by acting as detergents, and caveolin expression leads to the formation of detergent-resistant lipid rapid domains of the plasma membrane.

We found that ectopic expression of caveolin-1 increased the membrane content of cholesterol but in a threshold fashion in our cell lines (Figure 2). Apparently, the endog-

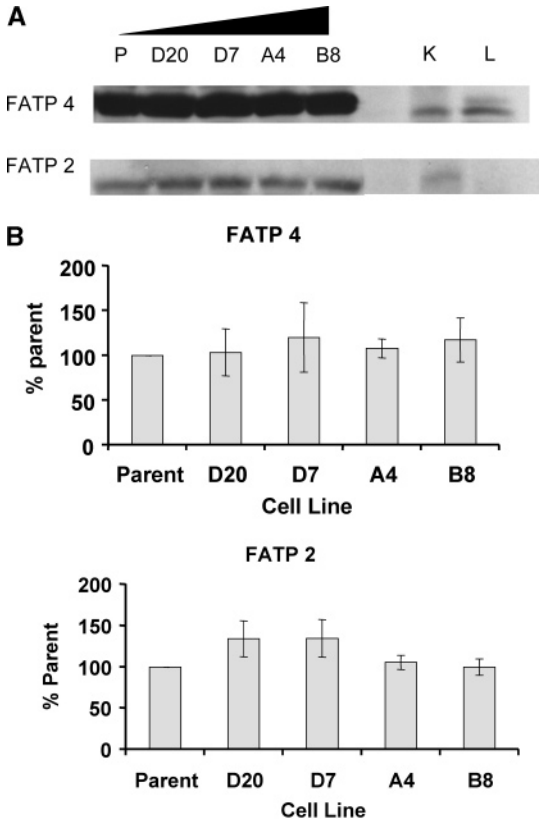

FIGURE 8: Expression of FATP2 and FATP4 is unaffected by caveolin-1 levels in HEK 293 cells. (A) Aliquots corresponding to equal amounts of protein were obtained from HEK cell membranes and subjected to SDS−PAGE and immunoblotted with the indicated antibodies. Detection was by a horseradish peroxidase-conjugated secondary antibody (Sigma) and an ECL substrate kit (New England Nuclear, Boston, MA). Shown is a representative blot of three experiments. (B) The gels were scanned, and band intensity was determined using an NIH image program; the results are expressed as arbitrary units (AU). The results are means ± standard deviations of three experiments. Kidney and lung from rat serve as controls.

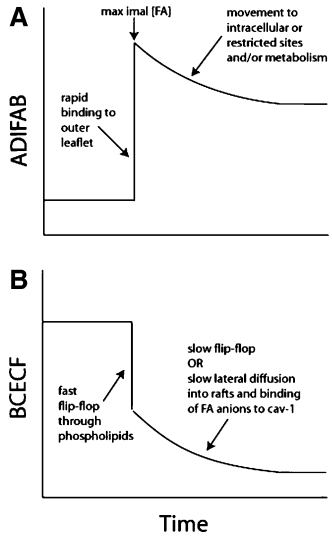

FIGURE 9: Schematic diagram of the changes in ADIFAB and BCECF fluorescence in HEK cells with high levels of expression of caveolin-1. Upon addition of a single dose of oleic acid, the fluorescence of ADIFAB increases to a maximal value as FA rapidly partition into the plasma membrane (A). BCECF fluorescence simultaneously decreases as FA rapidly flip-flop to the inner leaflet and release protons into the cytosol (B). The slow recovery of ADIFAB fluorescence represents (i) intracellular metabolism and (ii) sequestration of FA within ordered membrane domains or intracellular membranes. The additional slow phase of BCECF fluorescence decrease may represent (i) slow flip-flop of FA in ordered membrane regions, (ii) slow lateral diffusion out of these ordered regions followed by rapid flip-flop, or (iii) binding of ionized FA to caveolin-1 and the inwardly directed redistribution (flip-flop) of FA to the inner leaflet.

enous level of cholesterol found in the parental cell lines is sufficient to stabilize caveolin in the cell membrane up to a certain level of caveolin. However, when the level of caveolin expression in the transfected HEK 293 cells approaches that seen in adipocytes, which have one of the highest natural caveolin levels, additional cholesterol needs to be synthesized and directed to the cell surface. The threshold phenomenon for cholesterol levels correlated with the nature of the kinetics of transmembrane FA flux in different cell lines (Figure 3). All cell lines showed a very fast phase of transmembrane FA movement, but the high-caveolin/cholesterol level cells have a second slow phase of FA movement that can be equal in magnitude to the first phase (see below). The same kinetics are observed for FA with different structures: oleate, palmitate, and elaidate (Figure 5). During the 5−10 min time course of our FA flux measurements, only 10−20% of the added oleate is metabolized (Figure 7). CD36 is not present in these cells, and the levels of FATP2 and -4, the acylCoA ligase isoforms present in kidney but unlinked to hyperlipidemia, are unchanged in our HEK cell lines (Figure 8). Thus, we conclude that the observed modulation of transmembrane FA movement is a result of the increased cell surface caveolin/cholesterol content and not other potentially important factors such as the levels of CD36, FATP2, and FATP4 and altered FA metabolism.

The presence of caveolae in cells such as adipocytes can increase the available cell surface area without altering the size of the cell. This cannot account for the altered FA uptake kinetics we see in the high-caveolin-level-expressing HEK cells, since electron microscopy has revealed minimal, if any, caveolae in either parental or transfected cells (data not shown). The expression of caveolin-1 appears to be sufficient for formation of caveolae in some cells (*51*) but not others (*52*). Structural studies suggested that the expression of caveolin-1 oligomers can form arrays or rafts but that the expression of an additional protein(s) is likely to be required for the formation and maintenance of their cavelike morphology (*53*), consistent with our data.

What role then, if any, do proteins such as CD36 and FATP play in uptake of FA or specifically the transmembrane movement of FA? Mouse knockouts of CD36 and FATP1 have shown slower FA uptake in fat and muscle tissues where they are highly expressed (*54*, *55*). Conversely, when these proteins are ectopically expressed in cells, they enhance FA uptake (*56*). FATP1 is an acyl-CoA ligase (*57*) whose expression is likely to enhance FA uptake because it converts FA to fatty acyl-CoA, a molecule that cannot diffuse out of the cell (*21*), thus creating an inward-directed gradient that will drive FA transmembrane movement as suggested (*13*, *55*, *58*). However, the activity of FATP-1 and other acyl CoA ligases is not likely to affect the fast flip-flop, which is probably not a rate-limiting step in the overall uptake process. The mechanism(s) by which CD36 modulates membrane transport of FA is less clear than for FATP. CD36 is comprised of a large extracellular ω-like domain with the amino and carboxyl termini as the only transmembrane

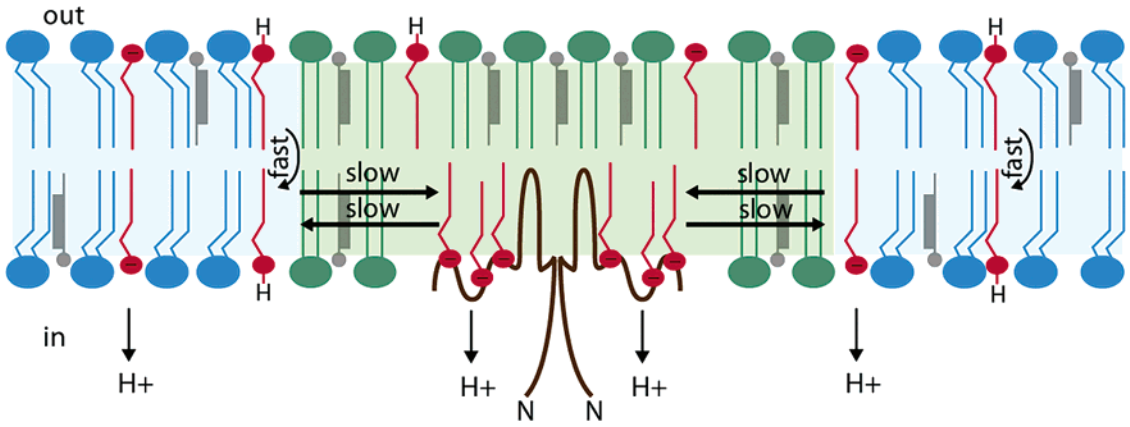

FIGURE 10: Proposed model (hypothesis) of fatty acid transport in membranes containing high levels of caveolin-1 and cholesterol. (A) FA rapidly bind and partition into liquid crystalline and gel phases of the membrane. (B) FA rapidly flip-flop through the liquid crystalline lipid phase but may flip-flop through the gel phase at a slower rate. (C) FA may diffuse rapidly into ordered membrane regions and become sequestered within these regions, which are more abundant in high-caveolin-level-expressing HEK cell lines. The lateral diffusion of FA may be slow within these domains such that the slow lateral diffusion of FA from the ordered phase into the liquid crystalline phase may limit the rate of FA flip-flip through the liquid crystalline phase. (D) Caveolin-1 may act as a sink for FA at the inner leaflet. The binding of fatty acid anions to caveolin-1 would deplete the amount of ionized FA in the lipid phase of the inner leaflet and generate an inwardly directed gradient favoring movement of additional FA to the inner leaflet.

segments (*59*); it does not resemble known transporters and apparently lacks enzymatic activity. CD36 functions as a lipoprotein receptor (*60*) and is targeted to adipocyte caveolae where it is highly enriched (*37*). Although this localization is generally consistent with hypotheses linking caveolae and FA uptake, this does not establish a mechanism for CD36 function.

On the other hand, our studies of controlled caveolin-1 expression in cells that do not normally express this protein allow us to postulate mechanisms by which caveolin-1 can affect FA transmembrane movement and trafficking. As shown in Figure 10, caveolin resides on the cytosolic leaflet of the plasma membrane. Upon addition of FA to the extracellular leaflet, FA can flip-flop rapidly across the lipid bilayer to reach the inner leaflet containing caveolin-1. The plasma membrane contains lipids both in disordered regions and ordered regions (e.g., rafts) containing large amounts of SM and cholesterol (*61*) and additional lipids such as plasmenylethanolamine (*62*), the levels of which are not expected to change with cholesterol (*62*). The higher degree of saturation in the acyl chains and the long saturated chain in the 1-position of SM allows the lipids in these regions to pack more tightly (*63*), which could decrease the rate of flip-flop of FA through these domains. Although, the rapid phase of acidification could reflect flip-flop across regions of higher mobility and the slower phase, flip-flop across regions of restricted mobility (Figures 9 and 10), preliminary data from our lab show that FA flip-flop is fast even in model membranes in highly ordered phases (K. Fontanini and J. A. Hamilton, unpublished data). Furthermore, the altered kinetics do not explain the larger pH decrease, which indicates that a larger amount of FA diffuses into the cytosolic leaflet of the plasma membrane of these cells and/or that the ionization of FA in the inner leaflet is altered.

We postulate three possible explanations for the additional, slow component of acidification: (i) binding of the FA to caveolin, which would sequester additional FA in the inner leaflet; (ii) an increased FA concentration in the inner leaflet by virtue of its partitioning into cholesterol-rich lipid raft domains, or a combination of these two mechanisms; and (iii) increased activity of acyl-CoA ligases.

The first possibility is considered most plausible because of the capacity of caveolin-1 to bind FA. FA binding sites within proteins such as albumin and the cytosolic FABPs are characterized by hydrophobic binding pockets near a patch of basic residues that form electrostatic interactions with the negatively charged FA carboxyl group (*64*). Therefore, we would expect that the ionized form of FA would bind to caveolin-1 and the membrane would serve as the hydrophobic pocket. There are 14 basic residues on caveolin-1, many of which would be situated adjacent to the surface of the inner lipid leaflet based on predicted topographic models of caveolin (*28*) (see Figure 10). Binding of FA to the protein at these sites would generate additional H^+ in the cytosol by two mechanisms: (i) re-ionization of the FA on the inner leaflet to compensate for the loss of FA anions in the lipid phase and (ii) equilibration of un-ionized FA from the outer leaflet (and release of protons) in response to the altered concentration gradient across the lipid bilayer. The rate of proton release might be limited by the relatively slow diffusion of FA to binding sites within the "raft" region in which caveolin-1 is located (Figure 10).

To evaluate our model (Figure 10), we must consider the amounts of FA and caveolin-1 in our experiments. We add 10 nmol of FA to the cuvette in a typical experiment, and our flip-flop model predicts that half of the FA will move to the inner leaflet and half of those FA (2.5 nmol) will release a proton. The slow phase of pH change is nearly equal in magnitude to the initial rapid pH change (Figure 3B), and therefore, this second phase also represents 2.0−2.5 nmol of FA. With one available FA binding site, 2.0−2.5 nmol of caveolin-1 would be required for the observed pH effect, and with binding to 10 binding sites, a 10-fold smaller amount of caveolin-1 would be needed. We utilize 2−3 mg of HEK cell protein per experiment, and we estimate the abundantly expressed caveolin-1 to comprise 0.2−0.4% of the total protein or 0.2−0.4 nM. Thus, a minimum of five FA binding sites per caveolin-1 molecule would support the

quantitative feasibility of our model (Figure 10), and there are five positively charged residues in the membrane-associated C-terminus and two in the N-terminus adjacent to the intramembranous sequence (*65*).

Caveolin could also influence the partitioning of FA into the inner leaflet indirectly by changing the environment to one more preferable to FA. With these results, this contribution cannot be discounted because the increased level of caveolin-1 expression is tightly associated with an increased level of cholesterol. To test this hypothesis, future work will attempt to rapidly deplete cholesterol from cells with a high level of caveolin 1 while leaving the plasma membrane intact, e.g., by exposure to β-methylcyclodextrin.

Two additional mechanisms that could contribute to a slow decrease in pH are (i) transmembrane movement of ionized FA and (ii) activity of acyl-CoA synthases in the plasma membrane. FA anions can flip-flop as a complex with a cation, with a rate much slower (3−4 orders of magnitude) than the rate of flip-flop of the un-ionized FA (*66*), although the rate can be enhanced by valinomycin (*67*). However, the net effect of FA anion flip-flop is to dissipate the pH gradient (*67*). On the other hand, conversion of FA to acyl-CoA on the cytosolic leaflet of the PM by FATP2 and FATP4, or by other acyl-CoA synthetases, would result in the inward flux of additional FA, which, according to the flip-flop mechanism, would deliver additional protons to the cytosolic compartment. Thus, the slow rate of acidification could reflect the limiting slow rate of enzyme activity. Caveolin-1 could stimulate the activity of ligases directly by a protein−protein interaction or indirectly by producing an altered lipid environment. However, the presence of caveolin-1 was not associated with an increased level of synthesis of di- and triglycerides (Figure 7), as most of the added FA remain unmetabolized in the time frame of our uptake measurements and there are no significant differences between the cell lines.

In summary, the level of caveolin-1 expression is correlated with membrane cholesterol levels in our HEK cell lines but has no effect on levels of FATP2 and -4, or on the synthesis of FAT/CD36 or other metabolic enzymes. Moreover, the kinetics of transmembrane FA movement are the same for three structurally distinct FA, *cis*-unsaturated, *trans*-unsaturated, and saturated. Taken together, these data lead us to conclude that diffusion is the primary mechanism of transport of FA into HEK cells and that caveolin and cholesterol increase the rate of transport of FA to the inner leaflet of the plasma membrane by modulating the biophysical properties of the membrane. Binding of FA in restricted regions, whether proteins or lipids, can trap the FA for a time scale that is significantly slower than that of flip-flop, thus preventing its immediate release into the cell. Such binding will also serve to sequester and concentrate reactants for metabolism of FA, the first step of which is activation to CoA derivatives. Although HEK cells have a relatively limited capability for metabolizing FA, compared to fat cells, for example, the sequestration mechanism could serve to enhance FA metabolism in other cells, since FA can be lost from cells by diffusion across fluid regions of the plasma membrane. Although our proposed (speculative) mechanisms may involve binding of FA to a protein in the plasma membrane, our new results also show that proteins are not required for the rapid influx of FA into HEK cells. Moreover, the general experimental approach applied here together with further manipulations of HEK cell protein content by transfection will allow us to make further determinations of the factors that affect transmembrane FA movement.

ACKNOWLEDGMENT

We thank Dr. Kellen Fontanini [Department of Biophysics, Boston University Medical Center (BUMC), Boston, MA] for help with Figure 10, Michael Gigliotti and Cheryl England (Department of Biophysics, BUMC) for performing the lipid analyses in Figures 3 and 7, and Dr. Christopher Pierce (Department of Pharmacology, BUMC) for help with statistical analysis.

REFERENCES

1. Brown, A. J., Jupe, S., and Briscoe, C. P. (2005) A family of fatty acid binding receptors, *DNA Cell Biol. 24*, 54−61.
2. Sampath, H., and Ntambi, J. M. (2004) Polyunsaturated fatty acid regulation of gene expression, *Nutr. Rev. 62*, 333−9.
3. Pownall, H. J., and Hamilton, J. A. (2003) Energy translocation across cell membranes and membrane models, *Acta Physiol. Scand. 178*, 357−65.
4. Kampf, J. P., and Kleinfeld, A. M. (2004) Fatty acid transport in adipocytes monitored by imaging intracellular free fatty acid levels, *J. Biol. Chem. 279*, 35775−80.
5. Trigatti, B. L., Anderson, R. G., and Gerber, G. E. (1999) Identification of caveolin-1 as a fatty acid binding protein, *Biochem. Biophys. Res. Commun. 255*, 34−9.
6. Bernlohr, D. A., Coe, N. R., and LiCata, V. J. (1999) Fatty acid trafficking in the adipocyte, *Semin. Cell Dev. Biol. 10*, 43−9.
7. Ibrahimi, A., and Abumrad, N. A. (2002) Role of CD36 in membrane transport of long-chain fatty acids, *Curr. Opin. Clin. Nutr. Metab. Care 5*, 139−45.
8. Luiken, J. J., Schaap, F. G., van Nieuwenhoven, F. A., van der Vusse, G. J., Bonen, A., and Glatz, J. F. (1999) Cellular fatty acid transport in heart and skeletal muscle as facilitated by proteins, *Lipids 34* (Suppl.), S169−75.
9. Schaffer, J. E., and Lodish, H. F. (1994) Expression cloning and characterization of a novel adipocyte long chain fatty acid transport protein, *Cell 79*, 427−36.
10. Hirsch, D., Stahl, A., and Lodish, H. F. (1998) A family of fatty acid transporters conserved from mycobacterium to man, *Proc. Natl. Acad. Sci. U.S.A. 95*, 8625−9.
11. Herrmann, T., Buchkremer, F., Gosch, I., Hall, A. M., Bernlohr, D. A., and Stremmel, W. (2001) Mouse fatty acid transport protein 4 (FATP4): Characterization of the gene and functional assessment as a very long chain acyl-CoA synthetase, *Gene 270*, 31−40.
12. Schmelter, T., Trigatti, B. L., Gerber, G. E., and Mangroo, D. (2004) Biochemical demonstration of the involvement of fatty acyl-CoA synthetase in fatty acid translocation across the plasma membrane, *J. Biol. Chem. 279*, 24163−70.
13. Pohl, J., Ring, A., Ehehalt, R., Herrmann, T., and Stremmel, W. (2004) New concepts of cellular fatty acid uptake: Role of fatty acid transport proteins and of caveolae, *Proc. Nutr. Soc. 63*, 259−62.
14. Kamp, F., Guo, W., Souto, R., Pilch, P. F., Corkey, B. E., and Hamilton, J. A. (2003) Rapid flip-flop of oleic acid across the plasma membrane of adipocytes, *J. Biol. Chem. 278*, 7988−95.
15. Kamp, F., and Hamilton, J. A. (1992) pH gradients across phospholipid membranes caused by fast flip-flop of un-ionized fatty acids, *Proc. Natl. Acad. Sci. U.S.A. 89*, 11367−70.
16. Hamilton, J. A., and Kamp, F. (1999) How are free fatty acids transported in membranes? Is it by proteins or by free diffusion through the lipids? *Diabetes 48*, 2255−69.
17. Hamilton, J. A., Johnson, R. A., Corkey, B., and Kamp, F. (2001) Fatty acid transport: The diffusion mechanism in model and biological membranes, *J. Mol. Neurosci. 16*, 99−108, 151−7 (discussion).
18. Doody, M. C., Pownall, H. J., Kao, Y. J., and Smith, L. C. (1980) Mechanism and kinetics of transfer of a fluorescent fatty acid between single-walled phosphatidylcholine vesicles, *Biochemistry 19*, 108−16.
19. Trigatti, B. L., and Gerber, G. E. (1996) The effect of intracellular pH on long-chain fatty acid uptake in 3T3-L1 adipocytes:

Evidence that uptake involves the passive diffusion of protonated long-chain fatty acids across the plasma membrane, *Biochem. J. 313* (Part 2), 487−94.
20. Zakim, D. (1996) Fatty acids enter cells by simple diffusion, *Proc. Soc. Exp. Biol. Med. 212*, 5−14.
21. Boylan, J. G., and Hamilton, J. A. (1992) Interactions of acyl-coenzyme A with phosphatidylcholine bilayers and serum albumin, *Biochemistry 31*, 557−67.
22. Pei, Z., Fraisl, P., Berger, J., Jia, Z., Forss-Petter, S., and Watkins, P. A. (2004) Mouse very long-chain Acyl-CoA synthetase 3/fatty acid transport protein 3 catalyzes fatty acid activation but not fatty acid transport in MA-10 cells, *J. Biol. Chem. 279*, 54454−62.
23. Carpentier, J. L., Perrelet, A., and Orci, L. (1976) Effects of insulin, glucagon, and epinephrine on the plasma membrane of the white adipose cell: A freeze-fracture study, *J. Lipid Res. 17*, 335−42.
24. Voldstedlund, M., Tranum-Jensen, J., and Vinten, J. (1993) Quantitation of Na^+/K^+-ATPase and glucose transporter isoforms in rat adipocyte plasma membrane by immunogold labeling, *J. Membr. Biol. 136*, 63−73.
25. Cohen, A. W., Razani, B., Wang, X. B., Combs, T. P., Williams, T. M., Scherer, P. E., and Lisanti, M. P. (2003) Caveolin-1-deficient mice show insulin resistance and defective insulin receptor protein expression in adipose tissue, *Am. J. Physiol. 285*, C222−35.
26. Scherer, P. E., Lisanti, M. P., Baldini, G., Sargiacomo, M., Mastick, C. C., and Lodish, H. F. (1994) Induction of caveolin during adipogenesis and association of GLUT4 with caveolin-rich vesicles, *J. Cell Biol. 127*, 1233−43.
27. Kandror, K. V., Stephens, J. M., and Pilch, P. F. (1995) Expression and compartmentalization of caveolin in adipose cells: Coordinate regulation with and structural segregation from GLUT4, *J. Cell Biol. 129*, 999−1006.
28. Cohen, A. W., Hnasko, R., Schubert, W., and Lisanti, M. P. (2004) Role of caveolae and caveolins in health and disease, *Physiol. Rev. 84*, 1341−79.
29. Rothberg, K. G., Heuser, J. E., Donzell, W. C., Ying, Y. S., Glenney, J. R., and Anderson, R. G. (1992) Caveolin, a protein component of caveolae membrane coats, *Cell 68*, 673−82.
30. Schnitzer, J. E., Oh, P., Pinney, E., and Allard, J. (1994) Filipin-sensitive caveolae-mediated transport in endothelium: Reduced transcytosis, scavenger endocytosis, and capillary permeability of select macromolecules, *J. Cell Biol. 127*, 1217−32.
31. Schnitzer, J. E., Allard, J., and Oh, P. (1995) NEM inhibits transcytosis, endocytosis, and capillary permeability: Implication of caveolae fusion in endothelia, *Am. J. Physiol. 268*, H48−55.
32. Henley, J. R., Krueger, E. W., Oswald, B. J., and McNiven, M. A. (1998) Dynamin-mediated internalization of caveolae, *J. Cell Biol. 141*, 85−99.
33. Oh, P., McIntosh, D. P., and Schnitzer, J. E. (1998) Dynamin at the neck of caveolae mediates their budding to form transport vesicles by GTP-driven fission from the plasma membrane of endothelium, *J. Cell Biol. 141*, 101−14.
34. Fielding, C. J., and Fielding, P. E. (2000) Cholesterol and caveolae: Structural and functional relationships, *Biochim. Biophys. Acta 1529*, 210−22.
35. Smart, E. J., Graf, G. A., McNiven, M. A., Sessa, W. C., Engelman, J. A., Scherer, P. E., Okamoto, T., and Lisanti, M. P. (1999) Caveolins, liquid-ordered domains, and signal transduction, *Mol. Cell. Biol. 19*, 7289−304.
36. Lisanti, M. P., Scherer, P. E., Vidugiriene, J., Tang, Z., Hermanowski-Vosatka, A., Tu, Y. H., Cook, R. F., and Sargiacomo, M. (1994) Characterization of caveolin-rich membrane domains isolated from an endothelial-rich source: Implications for human disease, *J. Cell Biol. 126*, 111−26.
37. Souto, R. P., Vallega, G., Wharton, J., Vinten, J., Tranum-Jensen, J., and Pilch, P. F. (2003) Immunopurification and characterization of rat adipocyte caveolae suggest their dissociation from insulin signaling, *J. Biol. Chem. 278*, 18321−9.
38. Vistisen, B., Roepstorff, K., Roepstorff, C., Bonen, A., van Deurs, B., and Kiens, B. (2004) Sarcolemmal FAT/CD36 in human skeletal muscle colocalizes with caveolin-3 and is more abundant in type 1 than in type 2 fibers, *J. Lipid Res. 45*, 603−9.
39. Wharton, J., Meshulam, T., Vallega, G., and Pilch, P. (2005) Dissociation of insulin receptor expression and signaling from caveolin-1 expression, *J. Biol. Chem. 280*, 13483−6.
40. Gross, D. N., Farmer, S. R., and Pilch, P. F. (2004) Glut4 storage vesicles without Glut4: Transcriptional regulation of insulin-dependent vesicular traffic, *Mol. Cell. Biol. 24*, 7151−62.
41. Tercyak, A. (1991) Determination of cholesterol and cholesterol esters, *J. Nutr. Biochem. 2*, 281−92.
42. Folch, J., Lees, M., and Sloane Stanley, G. H. (1957) A simple method for the isolation and purification of total lipides from animal tissues, *J. Biol. Chem. 226*, 497−509.
43. Sargiacomo, M., Scherer, P. E., Tang, Z., Kubler, E., Song, K. S., Sanders, M. C., and Lisanti, M. P. (1995) Oligomeric structure of caveolin: Implications for caveolae membrane organization, *Proc. Natl. Acad. Sci. U.S.A. 92*, 9407−11.
44. Fielding, C. J., Bist, A., and Fielding, P. E. (1999) Intracellular cholesterol transport in synchronized human skin fibroblasts, *Biochemistry 38*, 2506−13.
45. Lange, Y., and Ramos, B. V. (1983) Analysis of the distribution of cholesterol in the intact cell, *J. Biol. Chem. 258*, 15130−4.
46. Richieri, G. V., Ogata, R. T., and Kleinfeld, A. M. (1992) A fluorescently labeled intestinal fatty acid binding protein. Interactions with fatty acids and its use in monitoring free fatty acids, *J. Biol. Chem. 267*, 23495−501.
47. Malaud, E., Hourton, D., Giroux, L. M., Ninio, E., Buckland, R., and McGregor, J. L. (2002) The terminal six amino acids of the carboxy cytoplasmic tail of CD36 contain a functional domain implicated in the binding and capture of oxidized low-density lipoprotein, *Biochem. J. 364*, 507−15.
48. Kamp, F., Zakim, D., Zhang, F., Noy, N., and Hamilton, J. A. (1995) Fatty acid flip-flop in phospholipid bilayers is extremely fast, *Biochemistry 34*, 11928−37.
49. Guo, W., Huang, N., Cai, J., Xie, W., and Hamilton, J. A. (2005) Fatty acid transport and metabolism in HepG2 cells, *Am. J. Physiol.* (in press).
50. Razani, B., Combs, T. P., Wang, X. B., Frank, P. G., Park, D. S., Russell, R. G., Li, M., Tang, B., Jelicks, L. A., Scherer, P. E., and Lisanti, M. P. (2002) Caveolin-1-deficient mice are lean, resistant to diet-induced obesity, and show hypertriglyceridemia with adipocyte abnormalities, *J. Biol. Chem. 277*, 8635−47.
51. Fra, A. M., Williamson, E., Simons, K., and Parton, R. G. (1995) De novo formation of caveolae in lymphocytes by expression of VIP21-caveolin, *Proc. Natl. Acad. Sci. U.S.A. 92*, 8655−9.
52. Sowa, G., Pypaert, M., Fulton, D., and Sessa, W. C. (2003) The phosphorylation of caveolin-2 on serines 23 and 36 modulates caveolin-1-dependent caveolae formation, *Proc. Natl. Acad. Sci. U.S.A. 100*, 6511−6.
53. Fernandez, I., Ying, Y., Albanesi, J., and Anderson, R. G. (2002) Mechanism of caveolin filament assembly, *Proc. Natl. Acad. Sci. U.S.A. 99*, 11193−8.
54. Coburn, C. T., Knapp, F. F., Jr., Febbraio, M., Beets, A. L., Silverstein, R. L., and Abumrad, N. A. (2000) Defective uptake and utilization of long chain fatty acids in muscle and adipose tissues of CD36 knockout mice, *J. Biol. Chem. 275*, 32523−9.
55. Kim, J. K., Gimeno, R. E., Higashimori, T., Kim, H. J., Choi, H., Punreddy, S., Mozell, R. L., Tan, G., Stricker-Krongrad, A., Hirsch, D. J., Fillmore, J. J., Liu, Z. X., Dong, J., Cline, G., Stahl, A., Lodish, H. F., and Shulman, G. I. (2004) Inactivation of fatty acid transport protein 1 prevents fat-induced insulin resistance in skeletal muscle, *J. Clin. Invest. 113*, 756−63.
56. Abumrad, N., Coburn, C., and Ibrahimi, A. (1999) Membrane proteins implicated in long-chain fatty acid uptake by mammalian cells: CD36, FATP and FABPm, *Biochim. Biophys. Acta 1441*, 4−13.
57. Hall, A. M., Smith, A. J., and Bernlohr, D. A. (2003) Characterization of the acyl-CoA synthetase activity of purified murine fatty acid transport protein 1, *J. Biol. Chem. 278*, 43008−13.
58. Dirusso, C. C., Connell, E. J., Faergeman, N. J., Knudsen, J., Hansen, J. K., and Black, P. N. (2000) Murine FATP alleviates growth and biochemical deficiencies of yeast fat1Δ strains, *Eur. J. Biochem. 267*, 4422−33.
59. Abumrad, N. A., el-Maghrabi, M. R., Amri, E. Z., Lopez, E., and Grimaldi, P. A. (1993) Cloning of a rat adipocyte membrane protein implicated in binding or transport of long-chain fatty acids that is induced during preadipocyte differentiation. Homology with human CD36, *J. Biol. Chem. 268*, 17665−8.
60. Endemann, G., Stanton, L. W., Madden, K. S., Bryant, C. M., White, R. T., and Protter, A. A. (1993) CD36 is a receptor for oxidized low-density lipoprotein, *J. Biol. Chem. 268*, 11811−6.
61. Brown, D. A., and London, E. (1998) Functions of lipid rafts in biological membranes, *Annu. Rev. Cell Dev. Biol. 14*, 111−36.
62. Pike, L. J., Han, X., Chung, K. N., and Gross, R. W. (2002) Lipid rafts are enriched in arachidonic acid and plasmenylethanolamine and their composition is independent of caveolin-1 expression:

A quantitative electrospray ionization/mass spectrometric analysis, *Biochemistry 41*, 2075−88.

63. Guo, W., Kurze, V., Huber, T., Afdhal, N. H., Beyer, K., and Hamilton, J. A. (2002) A solid-state NMR study of phospholipid-cholesterol interactions: Sphingomyelin-cholesterol binary systems, *Biophys. J. 83*, 1465−78.
64. Hamilton, J. A. (2002) How fatty acids bind to proteins: The inside story from protein structures, *Prostaglandins, Leukotrienes Essent. Fatty Acids 67*, 65−72.
65. Kurzchalia, T. V., Dupree, P., Parton, R. G., Kellner, R., Virta, H., Lehnert, M., and Simons, K. (1992) VIP21, a 21-kD membrane protein is an integral component of trans-Golgi-network-derived transport vesicles, *J. Cell Biol. 118*, 1003−14.
66. Zeng, Y., Han, X., Schlesinger, P., and Gross, R. W. (1998) Nonesterified fatty acids induce transmembrane monovalent cation flux: Host−guest interactions as determinants of fatty acid-induced ion transport, *Biochemistry 37*, 9497−508.
67. Kamp, F., Hamilton, J. A., Kamp, F., Westerhoff, H. V., and Hamilton, J. A. (1993) Movement of fatty acids, fatty acid analogues, and bile acids across phospholipid bilayers, *Biochemistry 32*, 11074−86.

BI051999B